JOURNAL

OF THE AMERICAN CHEMICAL SOCIETY

© Copyright 1988 by the American Chemical Society

VOLUME 110, NUMBER 22 OCTOBER 26, 1988

Stereodynamics of *N*-Ethyl-*N*-methyl-2-aminobutane

Charles T. Danehey, Jr.,*,† Gilbert L. Grady,‡ Philippe R. Bonneau, and C. Hackett Bushweller*

Contribution from the Department of Chemistry, University of Vermont, Burlington, Vermont 05405. *Received December 14, 1987*

Abstract: *N*-Ethyl-*N*-methyl-2-aminobutane (EMAB) is the simplest acyclic trialkylamine which possesses a chiral carbon bonded to a chiral nitrogen. The chiral carbon is configurationally stable, while the chiral nitrogen is configurationally labile via nitrogen inversion. The ^1H dynamic NMR (DNMR) spectra of three selectively deuteriated derivatives of EMAB show a decoalescence into four subspectra with relative populations of 49%, 22%, 17%, and 12% at 104 K. The DNMR behavior can be simulated in terms of a model which involves a relatively high barrier for interconversion between diastereomers via nitrogen inversion ($\Delta G^{\ddagger}$ = 7.3 kcal/mol) and lower barriers for conformational interconversion via isolated rotation ($\Delta G^{\ddagger}$ = 6.4 and 5.6 kcal/mol). By using the NMR data and complementary molecular mechanics calculations, the 49% and 12% subspectra are assigned to conformations of the R_CR_N and S_CS_N stereoisomers, while the 22% and 17% subspectra are assigned to the R_CS_N and S_CR_N stereoisomers. Preferred conformations have the *N*-ethyl methyl group in one of the two positions gauche to the nitrogen lone pair, the C1 methyl of the 2-butyl group anti to the lone pair, and the C4 methyl of the 2-butyl group syn periplanar to the lone pair. There is no experimental evidence for conformations which have the methine proton or the *N*-ethyl methyl group anti to the lone pair.

When attempting to unravel the stereodynamics of a trialkylamine, one must remain cognizant of two fundamentally different types of internal motion, i.e., pyramidal inversion at nitrogen and isolated rotation about single bonds. The consequences of π-bonding, steric crowding, electronegativity, ring strain, and other structural parameters on the nitrogen inversion barrier are well-known.[1] Studies of isolated rotation about carbon–nitrogen single bonds and rotamer preferences by using microwave spectroscopy, infrared spectroscopy, Raman spectroscopy, and molecular orbital calculations have shed light on simple systems including methylamine,[2] dimethylamine,[2] trimethylamine,[2] ethylamine,[3] isopropylamine,[4] ethylmethylamine,[4b] and dimethylethylamine.[5] Recently, dynamic nuclear magnetic resonance (DNMR) spectroscopy at very low temperatures and molecular mechanics calculations revealed a comprehensive picture of the stereodynamics of diethylmethylamine,[6] triethylamine,[6,7] and tribenzylamine.[8]

Other efforts have focused on more crowded amines including *N*-ethyl-*N*-methyl-*N*-isopropylamine,[9] *N*-*tert*-butyl-*N*,*N*-dialkylamines,[10] *N*-*tert*-butyl-*N*-alkyl-*N*-haloamines,[11] and ever more crowded systems.[12] In light of the burgeoning interest in the chemistry of chiral systems, it is interesting to note that little attention has been focused on assessing the stereodynamics of chiral acyclic trialkylamines.

N-Ethyl-*N*-methyl-2-aminobutane (EMAB) is the simplest acyclic trialkylamine which possesses a chiral carbon bonded to a chiral nitrogen. There are four configurational stereoisomers of EMAB: R_CR_N, S_CS_N, R_CS_N, S_CR_N. The chiral carbon is configurationally stable. Facile nitrogen inversion renders the chiral nitrogen stereolabile and is sufficient to interconvert certain diastereomers (i.e., R_CR_N and R_CS_N, S_CR_N and S_CS_N). For each of the four stereoisomers, there is a family of 27 conformations which have staggered orientations about the N–CH_2, N–CH, and

† Current address: Union Carbide Corporation, Tarrytown, NY.
‡ Deceased.

(1) For excellent reviews, see: Rauk, A.; Allen, L. C.; Mislow, K. *Angew. Chem., Int. Ed. Engl.* **1970**, 9, 400. Lambert, J. B. *Top. Stereochem.* **1971**, *6*, 19. Lehn, J. M. *Fortschr. Chem. Forsch.* **1970**, *15*, 311. Payne, P. W.; Allen, L. C. In *Applications of Electronic Structure Theory*; Schaefer, H. F., Ed.; Plenum Press: New York, 1977; Vol. 4.

(2) Tsuboi, M.; Hirakawa, A. Y.; Tamagake, K. *J. Mol. Spectrosc.* **1967**, *22*, 272. Nishikawa, T.; Itoh, T.; Shimoda, K. *J. Chem. Phys.* **1955**, *23*, 1735. Flood, E.; Pulay, P.; Boggs, J. E. *J. Am. Chem. Soc.* **1977**, *99*, 5570. Wollrab, J. W.; Laurie, V. W. *J. Chem. Phys.* **1968**, *48*, 5058. Erlandson, G.; Gurdy, W. *Phys. Rev.* **1957**, *106*, 513. Lide, D. R., Jr.; Mann, D. E. *J. Chem. Phys.* **1958**, *28*, 572.

(3) Durig, J. R.; Li, Y. S. *J. Chem. Phys.* **1975**, *63*, 4110. Tsuboi, M.; Tamagake, K.; Hirakawa, A. Y.; Yamaguchi, J.; Nakagava, H.; Manocha, A. S.; Tuazon, E. C.; Fateley, W. G. *J. Chem. Phys.* **1975**, *63*, 5177.

(4) (a) Krueger, P. J.; Jan, J. *Can. J. Chem.* **1970**, *48*, 3229. (b) Durig, J. R.; Compton, D. A. C. *J. Phys. Chem.* **1979**, *83*, 2873.

(5) Durig, J. R.; Cox, F. O. *J. Mol. Struct.* **1982**, *95*, 85.

(6) Bushweller, C. H.; Fleischman, S. H.; Grady, G. L.; McGoff, P.; Rithner, C. D.; Whalon, M. R.; Brennan, J. G.; Marcantonio, R. P.; Domingue, R. P. *J. Am. Chem. Soc.* **1982**, *104*, 6224.

(7) Fleischman, S. H.; Weltin, E. E.; Bushweller, C. H. *J. Computat. Chem.* **1985**, *6*, 249.

(8) Fleischman, S. H.; Whalon, M. R.; Rithner, C. D.; Grady, G. L.; Bushweller, C. H. *Tetrahedron Lett.* **1982**, *23*, 4233. See, also: Bushweller, C. H.; O'Neil, J. W. *J. Am. Chem. Soc.* **1970**, *92*, 2159. Bushweller, C. H.; O'Neil, J. W.; Bilofsky, H. S. *Tetrahedron* **1972**, *28*, 2697.

(9) Bushweller, C. H.; Wang, C. Y.; Reny, J.; Lourandos, M. Z. *J. Am. Chem. Soc.* **1977**, *99*, 3938.

(10) Bushweller, C. H.; Anderson, W. G.; Stevenson, P. E.; Burkey, D. L.; O'Neil, J. W. *J. Am. Chem. Soc.* **1974**, *96*, 3892.

(11) Bushweller, C. H.; Anderson, W. G.; Stevenson, P. E.; O'Neil, J. W. *J. Am. Chem. Soc.* **1975**, *97*, 4338.

(12) Lunazzi, L.; Macciantelli, D.; Grossi, L. *Tetrahedron* **1983**, *39*, 305. Berger, P. A.; Hobbs, C. F. *Tetrahedron Lett.* **1978**, 1905.

0002-7863/88/1510-7269$01.50/0 © 1988 American Chemical Society

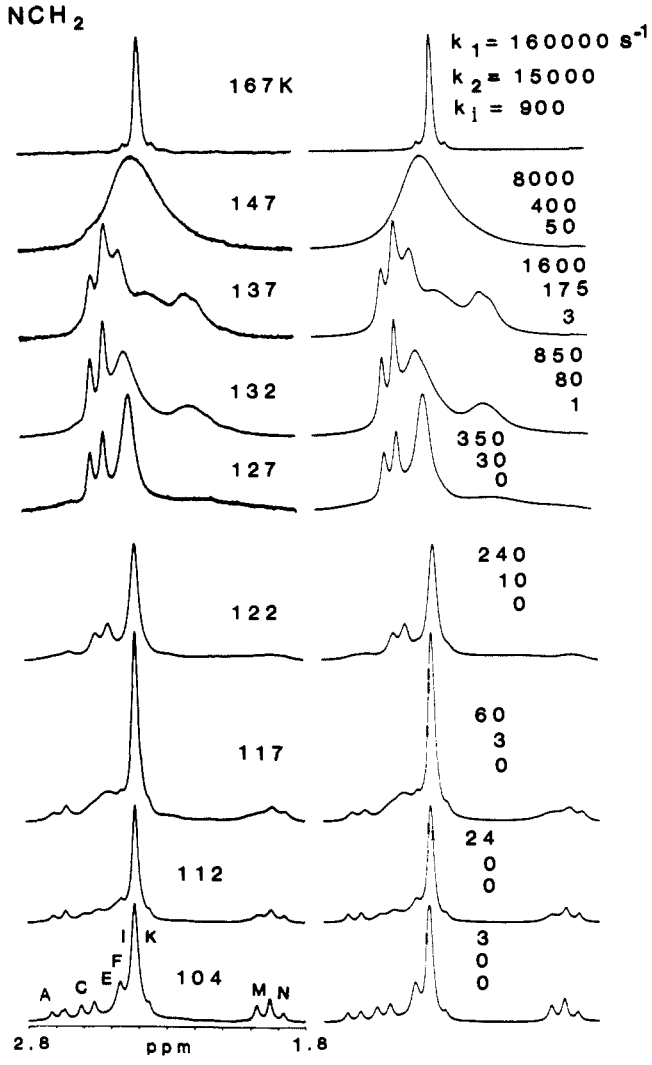

Figure 1. Experimental ^{1}H DNMR spectra (250 MHz) of the NCH_2 protons of **1** (3% v/v in $CBrF_3$) at various temperatures (left column) and theoretical simulations (right column). k_i is the first-order rate constant for inversion at nitrogen. k_1 is the rate constant for isolated rotation which converts the R_CS_N/S_CR_N GAG′ and GAG family of conformations to the G′GG and GGG family. k_2 is the rate constant for isolated rotation which converts the R_CR_N/S_CS_N G′AG′, GAG′, G′AG, and GAG family of conformations to the GG′G conformation. See Table II and Scheme I.

$CH-CH_2$ bonds. The R_CR_N and S_CS_N families are enantiomeric. The R_CS_N and S_CR_N families are also enantiomeric. The R_CR_N and R_CS_N families are diastereomeric as are the S_CS_N and S_CR_N species. Thus, in achiral solvents, there are, in principle, 54 NMR distinguishable conformations of EMAB.

This report concerns complementary ^{1}H DNMR and molecular mechanics studies of EMAB which reveal the presence of 18 equilibrium conformations which are present at concentrations high enough to be NMR detectable. The DNMR studies also allow elucidation of conformational exchange itineraries via nitrogen inversion and isolated rotation.

^{1}H DNMR Studies. The ^{1}H DNMR spectrum (250 MHz) of EMAB (3% v/v in $CBrF_3$) from 200 to 100 K shows obvious decoalescence behavior, but multiple overlapping subspectra at very low temperatures preclude a facile interpretation. Therefore, we examined the simplified ^{1}H DNMR spectra of the three selectively deuteriated derivatives of EMAB below.

	RR′NR″		
compd	R	R′	R″
1	CD_3CH_2	CD_3	$CD_3CDCD_2CH_3$
2	CH_3CD_2	CH_3	$CD_3CHCD_2CH_3$
3	CD_3CD_2	CD_3	$CH_3CHCH_2CD_3$

Table I. ^{1}H NMR Parameters for the NCH_2CD_3 and CD_2CH_3 Subspectra of Compound **1** at 104 K[a]

subspectral population, %	chemical shifts of NCH_2CD_3, ppm ($^2J_{HH}$, Hz)	chemical shift of CD_2CH_3,[b] ppm
49	δ_I 2.43, δ_K 2.40 (−13)	δ_W 0.96
12	δ_A 2.69, δ_N 1.90 (−12)	δ_Z 0.84
22	δ_C 2.58, δ_M 1.95 (−12)	δ_X 0.95
17	δ_E 2.48, δ_F 2.45 (−11)	δ_Y 0.86

[a] Subscripts at the beginning of the alphabet denote high-frequency signals (e.g., δ_A). Subscripts near the end of the alphabet denote low-frequency signals. [b] Singlet resonances.

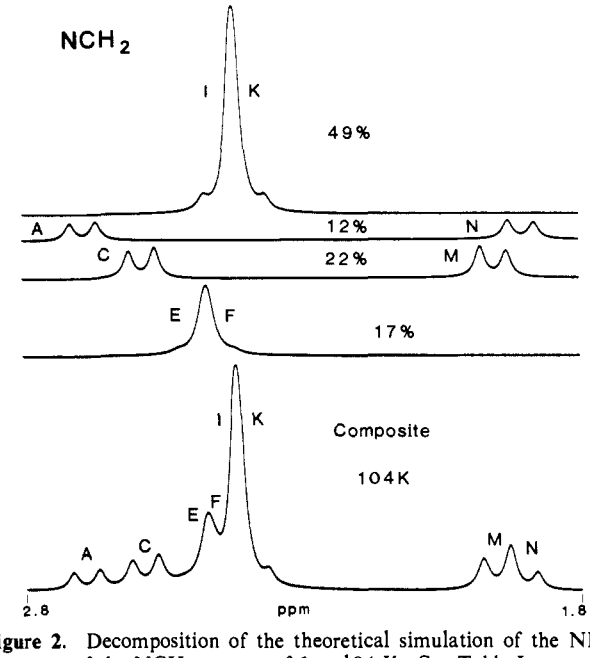

Figure 2. Decomposition of the theoretical simulation of the NMR spectrum of the NCH_2 protons of **1** at 104 K. See Table I.

Compound 1. The ^{1}H NMR spectrum of the NCH_2 group of **1** (3% v/v in $CBrF_3$) at 167 K *and above* is a closely spaced AB spectrum (δ_A 2.40, δ_B 2.33; $^2J_{AB}$ = −11 Hz) as shown in Figure 1. At 167 K, nitrogen inversion and all isolated rotation processes are fast on the NMR chemical exchange time scale.[6] The methylene protons are diastereotopic by virtue of the molecular asymmetry generated by the chiral methine carbon.[13] Below 167 K, the spectrum undergoes a complex decoalescence. Slow-exchange conditions are achieved at 104 K (Figure 1). The spectrum at 104 K can be simulated accurately by superimposing four two-spin subspectra (IK, AN, CM, EF) of unequal populations (49%, 12%, 22%, 17%).[14] The spectrum at 104 K is decomposed in Figure 2, and NMR parameters are compiled in Table I.

In order to achieve accurate theoretical simulations of the exchange-broadened spectra between 104 and 127 K, just two spin-system exchanges are allowed: CM with EF, IK with AN. *No other magnetization transfers are allowed.* In Figure 1, rate constant k_1 is associated with the CM to EF exchange and k_2 with the IK to AN process. Free energies of activation and assigned conformational interconversions (vide infra) are compiled in Table II. Above 127 K, it was necessary to include four additional spin-system exchanges in order to achieve accurate line fits: IK with MC, IK with FE, AN with MC, AN with FE. The rate constant k_i in Figure 1 is associated with each of the IK to MC, IK to FE, AN to MC, and AN to FE processes. We found that the use of equal rate constants for all four of these processes was sufficient to give excellent spectral fits (Figure 1).

With use of a rationale that has been discussed in detail previously,[6,10] k_i is the rate constant associated with *nitrogen inversion*,

(13) Mislow, K.; Raban, M. *Top. Stereochem.* **1967**, *1*, 1.
(14) Bushweller, C. H.; Letendre, L. J.; Brunelle, J. A.; Bilofsky, H. S.; Whalon, M. R.; Fleischman, S. H. *QCPE* **1983**, 466.

Table II. Activation Parameters for Conformational Interconversion in Compound **1** Derived from Simulations of the NCH_2CD_3 ^1H DNMR Spectra

magnetizatn transfer[a]	rate constant[b]	$\Delta G^{\ddagger}$, kcal/mol (temp, K)	conformatnal interconvrsn[c]
CM to EF	k_1	5.6 ± 0.2 (122)	R_CS_N or S_CR_N stereoisomers: (GAG', GAG) to (GGG, G'GG)
IK to AN	k_2	6.4 ± 0.2 (122)	R_CR_N or S_CS_N stereoisomers: (G'AG', GAG', G'AG, GAG) to (GG'G)
IK to MC			inversion at nitrogen:
IK to FE	k_i	7.3 ± 0.2 (147)	
AN to MC			R_CR_N to R_CS_N
AN to FE			S_CS_N to S_CR_N

[a] See Table I and Figure 2. [b] See Figure 1. [c] Parentheses denote a family of conformations which are undergoing rapid interconversion via isolated rotation at 104 K. See Scheme I.

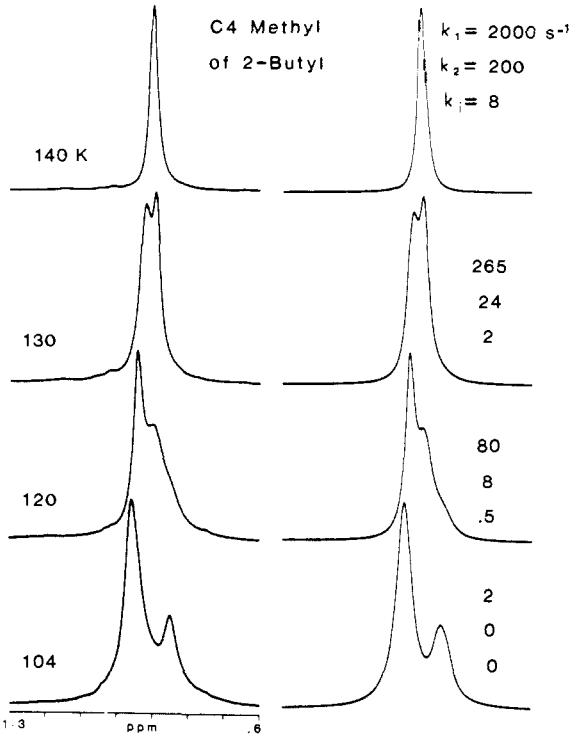

Figure 3. Experimental ^1H DNMR spectra of the C4 methyl group of the 2-butyl group of **1** at various temperatures (left column) and theoretical simulations (right column). The rate constants are defined in the caption to Figure 1.

i.e., interconversion between diastereomers R_CR_N and R_CS_N or between S_CS_N and S_CR_N. Rate constants k_1 and k_2 are associated with lower barrier *isolated rotation* processes occurring within each of the diastereomeric families of conformations.[6]

The ^1H NMR spectrum of the C4 methyl of the 2-butyl group of **1** is a singlet at 150 K and above. At 130 K, the C4 signal is decoalesced into two overlapping singlets consistent with slowing nitrogen inversion (Figure 3), i.e., slowing interconversion between diastereomers. Below 130 K, the spectrum decoalesces again consistent with slowing isolated rotation processes. In order to achieve an adequate fit of the slow-exchange spectrum at 104 K *and* adequate internally consistent fits of the exchange-broadened spectra above 104 K, we were required to employ four singlets in the DNMR simulation model at δ_W 0.96 (49%), δ_Z 0.84 (12%), δ_X 0.95 (22%), and δ_Y 0.86 (17%). The 104 K spectrum is decomposed in Figure 4. From 104 to 130 K, the only allowed chemical shift exchanges are resonance W with Z and X with Y (Figure 3). As in the case of the NCH_2 resonance, additional exchanges are required above 130 K to account for the onset of nitrogen inversion. The subspectral populations for the C4 methyl

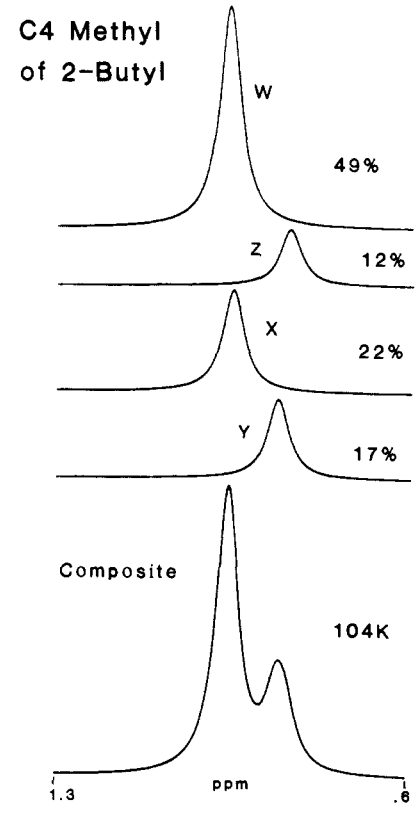

Figure 4. Decomposition of the theoretical simulation of the NMR spectrum of the C4 methyl protons of the 2-butyl group of **1** at 104 K. See Table I.

Table III. ^1H NMR Parameters for the NCH, NCH_3, and NCD_2CH_3 Subspectra of Compound **2** at 104 K[a]

subspectral population, %	chemical shift of NCH, ppm	chemical shift of NCH_3, ppm
49	δ_A 2.70	δ_N 2.08
12	δ_E 2.47	δ_K 2.29
22	δ_F 2.43	δ_L 2.25
17	δ_B 2.69	δ_M 2.10

[a] The NCD_2CH_3 spectrum consists of four overlapping singlets in the narrow chemical shift range δ 1.04 to δ 1.09.

resonance at 104 K and the free energies of activation for the W to Z (6.3 ± 0.2 kcal/mol), X to Y (5.8 ± 0.2 kcal/mol), and inversion (7.4 ± 0.2 kcal/mol) processes agree well with the correspondingly populated NCH_2 subspectra and corresponding free energies of activation (Tables I and II).

Compound 2. The ^1H NMR spectrum of **2** (3% v/v in $CBrF_3$) at 160 K shows singlet resonances for the NCH and NCH_3 moieties (Figure 5). At 130 K, each resonance has separated into two signals consistent with slowing nitrogen inversion. Below 130 K, additional decoalescence occurs due to slowing isolated rotations, and a slow-exchange spectrum is achieved at 104 K. In order to achieve accurate internally consistent fits of the NCH spectrum at 104 K *and* the exchange-broadened spectra up to 160 K, it was necessary to employ four singlets in the DNMR simulation model at δ_A 2.70 (49%), δ_B 2.69 (17%), δ_E 2.47 (12%), and δ_F 2.43 (22%). The NCH spectrum at 104 K is decomposed in Figure 6, and NMR parameters are compiled in Table III. The NCH_3 resonance is also simulated accurately by using four singlets (Table III). Once again, there is strong agreement between subspectral populations at 104 K for the NCH and NCH_3 resonances of **2** and the NCH_2 resonances of **1** (Tables I and III). In addition, there is a strong consistency among the free energies of activation for transfers of magnetization between correspondingly populated subspectra in **1** and **2**. In **2**, the $\Delta G^{\ddagger}$ values for the F to B (or L to M), A to E (or N to K), and inversion processes are 5.6, 6.3, and 7.4 kcal/mol, respectively (See Table II for comparison with **1**).

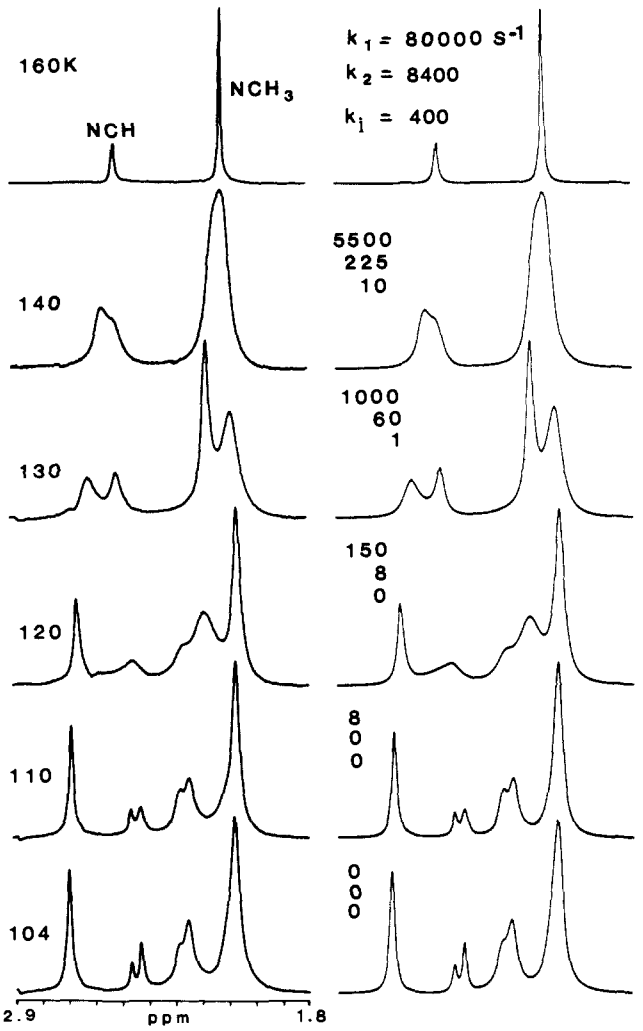

Figure 5. Experimental ^1H DNMR spectra of the NCH and NCH_3 protons of **2** at various temperatures (left column) and theoretical simulations (right column). The rate constants are defined in the caption to Figure 1.

In light of the substantial dependence of the chemical shift of an NCH proton on the orientation of the proton vis-ã-vis the nitrogen lone pair,[6] it is noteworthy that the NCH chemical shifts of **2** at 104 K occur in a narrow 0.27-ppm range. This suggests that, in *all* of the NMR detectable conformations of **2**, the methine proton is either gauche *or* anti to the lone pair, i.e., it cannot be gauche in one conformation and anti in the others or vice versa.

The 2-butyl C4 methyl resonance of **2** decoalesces in a manner identical with that in **1**. The NCD_2CH_3 resonance of **2** shows evidence of decoalescence at 104 K into very closely spaced singlets. An adequate simulation of the spectrum at 104 K was achieved by using four overlapping singlets in the narrow chemical shift range from δ 1.09 to δ 1.04. *This chemical shift range is highly characteristic of an N-ethyl methyl group which is oriented gauche to the lone pair.*[6,10]

Compound 3. The ^1H NMR spectrum of **3** (3% v/v in $CBrF_3$) at 200 K shows an $AKMX_3$ spectrum (δ_A 2.50, δ_K 1.59, δ_M 1.20, δ_X 0.91; $^3J_{AK}$ = 2 Hz, $^3J_{AM}$ = 12 Hz, $^3J_{AX}$ = 6 Hz, $^2J_{KM}$ = −13 Hz, $^4J_{KX} \cong {}^4J_{MX} \cong 0$ Hz). The methine proton and the methyl protons give the signals at δ_A 2.50 and δ_X 0.91, respectively. The two multiplets at δ_K 1.59 and δ_M 1.20 are due to the diastereotopic methylene protons. The spectrum from δ 1.90 to δ 0.50 is illustrated in Figure 7. At temperatures below 200 K, decoalescence occurs, and slow exchange is achieved at 104 K.

The spectra in Figure 7 result from an overlapping of subspectra due to the methylene and methyl protons. At 104 K, resolution of the scalar coupling for each of the methyl doublets is not observed due to line broadening resulting from efficient transverse relaxation (T_2) at a low temperature in a viscous solvent. Excellent

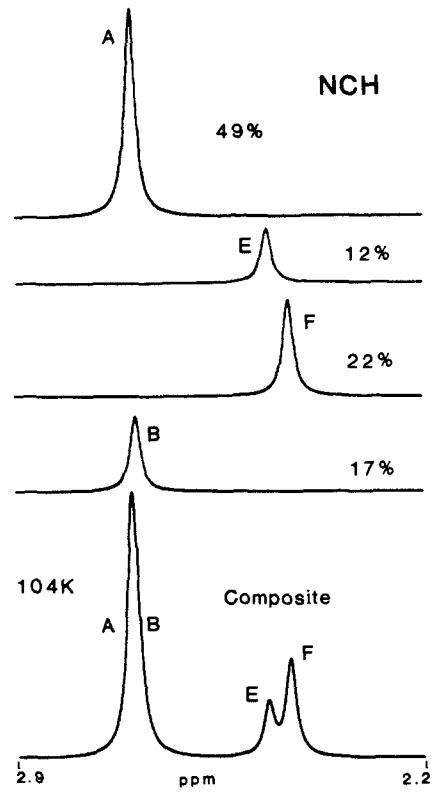

Figure 6. Decomposition of the theoretical simulation of the NMR spectrum of the NCH proton of **2** at 104 K. See Table III.

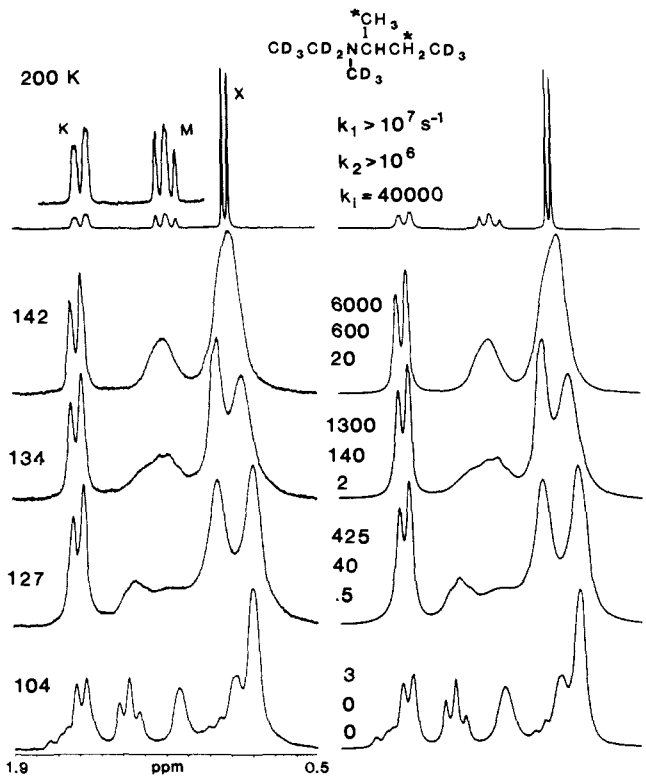

Figure 7. Experimental ^1H DNMR spectra of the C1 methyl and methylene protons of the 2-butyl group of **3** at various temperatures (left column) and theoretical simulations (right column). Rate constants are defined in the caption of Figure 1. See Table VI.

fits of the DNMR spectra are obtained by using a three-spin model ($CHCH_2$) to simulate the subspectrum of the methylene protons (CH_2) which show scalar coupling to the methine proton (CH) and superimposing this on the methyl protons subspectrum calculated by using a four-spin ($CHCH_3$) model. The approximation

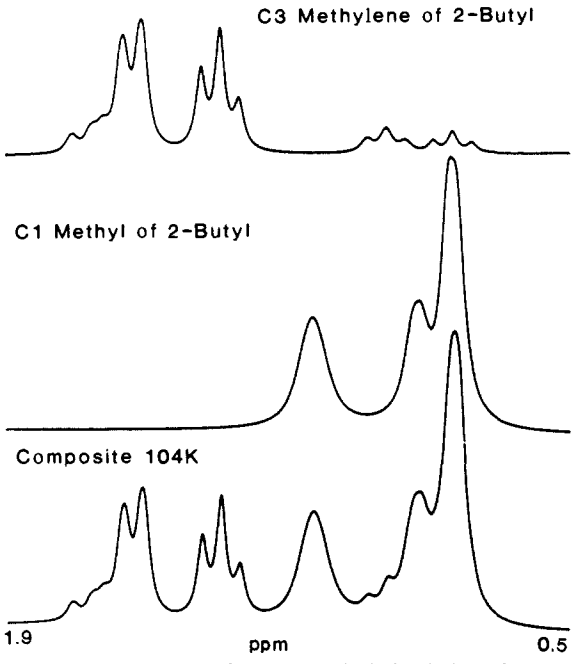

Figure 8. Decomposition of the theoretical simulation of the NMR spectrum of **3** at 104 K into methylene and methyl protons subspectra.

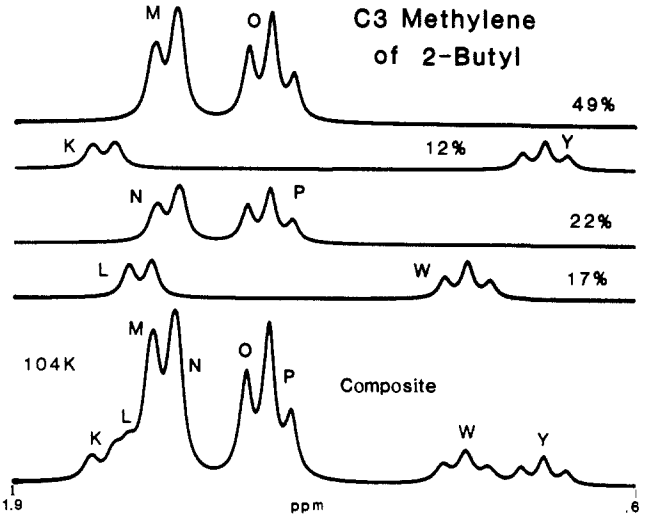

Figure 9. Decomposition of the theoretical simulation of the NMR spectrum of the methylene protons of **3** at 104 K. See Table IV.

in these simplified models is that $^4J_{HH}$ values are negligible. Indeed, this was verified by performing a rigorous six-spin simulation of the spectrum at 104 K.[15]

The methylene protons spectrum at 104 K is simulated accurately by employing four subspectra. The composite methylene protons spectrum is shown at the top of Figure 8. This spectrum is decomposed in Figure 9 with NMR parameters compiled in Table IV. Subspectral populations agree with those for compounds **1** and **2** (Tables I–III). It is noteworthy that, for each of the four subspectra, the two $^3J_{HH}$ values are very different. This means that, for each case, one of the methylene protons is predominantly anti to the methine proton ($^3J_{HH}$ = 12 Hz) and the other gauche to the methine proton ($^3J_{HH} \cong$ 3 Hz).

The methyl protons spectrum of **3** at 104 K was simulated by using four four-spin ($CHCH_3$) subspectra. The composite spectrum is shown in Figure 8 and is decomposed in Figure 10. NMR parameters are compiled in Table V. Superposition of the composite spectra from Figures 9 and 10 results in an excellent fit to the experimental spectrum at 104 K. In addition, the free energies of activation derived from DNMR line shape analyses for **3** (Figure 7; Table VI) correlate well with those for compounds **1** and **2**.

Thus, compounds **1–3** consistently show four subspectra at 104 K with relative populations of 49%, 22%, 17%, and 12%. Each subspectrum contains information regarding the identity of the conformation or family of conformations which gives that subspectrum.

Assignment of Conformations. If the absolute configuration at nitrogen and at the methine carbon of EMAB is specified, the three-letter designation summarized in Table VII is sufficient to name any staggered conformation of a given stereoisomer. We

(15) Johannesen, R. B.; Ferretti, J. A.; Harris, R. K. *QCPE* **1985**, 188.

Table IV. ^{1}H NMR Parameters for the Methylene Protons of Compound **3** at 104 K

subspectral population, %	chemical shifts of methylene protons, ppm	chemical shift of methine proton,[a] ppm	coupling constants, Hz
49	δ_M 1.58, δ_O 1.37	δ_A 2.70	$^3J_{AM}$ = 3, $^3J_{AO}$ = 12
			$^2J_{MO}$ = −12
12	δ_K 1.71, δ_Y 0.79	δ_E 2.47	$^3J_{EK}$ = 3, $^3J_{EY}$ = 12
			$^2J_{KY}$ = −12
22	δ_N 1.58, δ_P 1.37	δ_F 2.43	$^3J_{FN}$ = 3, $^3J_{FP}$ = 12
			$^2J_{NP}$ = −12
17	δ_L 1.64, δ_W 0.95	δ_B 2.69	$^3J_{BL}$ = 2, $^3J_{BW}$ = 12
			$^2J_{LW}$ = −12

[a] Determined from spectrum of **2** at 104 K (Table III).

Table V. ^{1}H NMR Parameters for the CH_3 Group of **3** at 104 K

subspectral population	chemical shift of CH_3, ppm ($^3J_{HH}$, Hz)[a]	subspectral population	chemical shift of CH_3, ppm ($^3J_{HH}$, Hz)[a]
49%	δ_Z 0.79 ($^3J_{AZ}$ = 6)	22%	δ_X 0.88 ($^3J_{FX}$ = 6)
12%	δ_R 1.15 ($^3J_{ER}$ = 6)	17%	δ_S 1.12 ($^3J_{BS}$ = 6)

[a] $^3J_{HH}$ is the scalar coupling constant to the methine proton at δ_A 2.70, δ_E 2.47, δ_F 2.43, δ_B 2.69 (Table III).

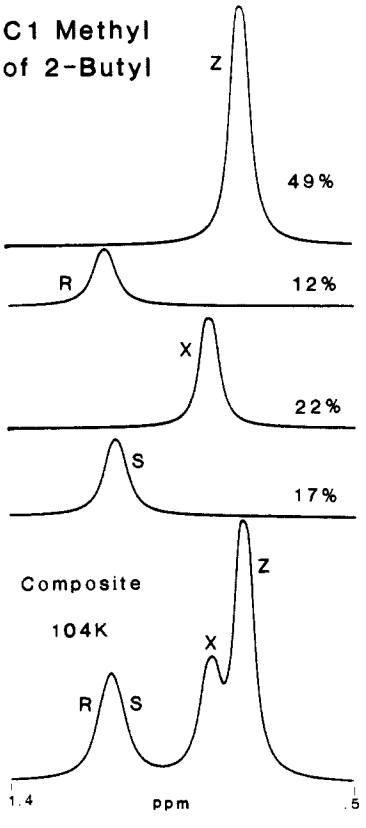

Figure 10. Decomposition of the theoretical simulation of the NMR spectrum of the methyl protons of **3** at 104 K. See Table V.

Table VI. Activation Parameters for Conformational Interconversion in Compound **3** Derived from Simulations of the Superimposed CH_2 and CH_3 Spectra

magnetizatn transfer	rate constant[c]	$\Delta G^{\ddagger}$, kcal/mol (temp, K)	conformatnal interconvrsn[d]
FNP to BLW[a] FX_3 to BS_3[b]	k_1	5.7 ± 0.2 (127)	R_CS_N or S_CR_N stereoisomers: (GAG', GAG) to (GGG, G'GG)
AMO to EKY[a] AZ_3 to ER_3[b]	k_2	6.3 ± 0.2 (127)	R_CR_N or S_CS_N stereoisomers: (G'AG', GAG', G'AG, GAG) to (GG'G)
AMO to FPN[a] AMO to BWL[a] EKY to FPN[a] EKY to BWL[a] AZ_3 to FX_3[b] AZ_3 to BS_3[b] ER_3 to FX_3[b] ER_3 to BS_3[b]	k_i	7.3 ± 0.2 (147)	inversion at nitrogen R_CR_N to R_CS_N S_CS_N to S_CR_N

[a] CH_2 spectra. [b] CH_3 spectra. [c] See Figure 7. [d] See footnote *c* in Table II.

Table VII. The Three-Letter Designation for Naming Conformations of EMAB

letter	orientation[a]
First Letter (Orientation of *N*-Ethyl Methyl)	
G	methyl gauche to LP and *N*-methyl
G'	methyl gauche to LP and 2-butyl
A	methyl anti to LP
Second Letter (Orientation of C1 Methyl of 2-Butyl)	
G	gauche to LP and *N*-methyl
G'	gauche to LP and *N*-ethyl
A	anti to LP
Third Letter (Orientation of C4 Methyl of 2-Butyl)	
G	gauche to methine proton and C1 methyl
G'	gauche to methine proton and nitrogen
A	anti to methine proton

[a] LP = nitrogen lone pair electrons.

will use the three-letter nomenclature system in Table VII.

If the NMR data above are used to deduce conformational preferences, some well-established trends in ^1H NMR chemical shifts and rotation barriers for acyclic trialkylamines are useful. These are summarized below.

(a) For the $NCCH_3$ moiety, the methyl protons resonance occurs at δ 1.10 ± 0.06 if the methyl group is gauche to the nitrogen lone pair (LP) and at δ 0.85 ± 0.06 if anti to the LP.[6,10]

(b) For the NCH_2 moiety, if one proton is gauche to the LP and the other anti, the chemical shift difference is normally large (i.e., 0.6–1.0 ppm). If both protons are gauche to the LP, the chemical shift difference is usually small (e.g., 0.0–0.3 ppm).[6,10]

(c) If a methyl group and the LP are separated by three atoms (including nitrogen) and are syn periplanar to each other, the ^1H chemical shift of the methyl protons tends to be shifted to a higher frequency than that for other orientations. For example, in the monoaxial conformation of *N,N',N''*-trimethyl-1,3,5-triazane, the axial methyl protons chemical shift is at δ 2.58 and the equatorial methyl protons chemical shift is at δ 1.94.[16]

(d) The rotation barrier about the N–CH_2 bond of an *N*-ethyl group via the itinerary during which methyl eclipses the LP is 4.4 kcal/mol.[6] This process is fast on the NMR chemical exchange time scale even at 100 K and therefore is DNMR-invisible above 100 K. Thus, for EMAB, a direct G to G' equilibration for *N*-ethyl methyl is DNMR-invisible above 100 K. If the G and G' orientations are comparably populated, the NCH_2 protons chemical shifts will be time-averaged at 100 K to a zero or small chemical shift difference. In contrast, rotation about the N–CH_2 bond during which methyl eclipses another alkyl group (e.g., G to A or G' to A conversions) has a barrier of ~6 kcal/mol and is slow enough to be DNMR-visible above 100 K.[6]

A perusal of Tables I, III, IV, and V shows excellent agreement among subspectral populations for compounds **1**, **2**, and **3** at 104 K. Each compound produces four subspectra with relative populations of 49%, 12%, 22%, and 17%. The highest temperature decoalescence (Figures 1, 3, 5, and 7) is assigned to slowing interconversion between diastereomers via nitrogen inversion. *Diastereomeric interconversion is slow at 130 K.* Below 130 K, nitrogen inversion no longer affects the DNMR line shape. Decoalescence below 130 K is assigned to isolated rotation processes which interconvert conformations within each of the two diastereomeric R_CR_N/S_CS_N and R_CS_N/S_CR_N families of conformations. Below 130 K, accurate DNMR line shape simulations invoked just two transfers of magnetization, i.e., exchange of the 49% subspectrum with the 12% subspectrum and 22% with 17% (Tables II and VI). *Therefore, the 49% and 12% subspectra belong to the NMR-detectable conformations of one set of enantiomeric stereoisomers (e.g., R_CR_N and S_CS_N), and the 22% and 17% subspectra are due to the diastereomeric counterparts* (e.g., R_CS_N and S_CR_N). It remains to assign subspectra to specific diastereomers and to the NMR-detectable conformations of these diastereomers.

49% Subspectrum. The 49% subspectrum of the NCH_2CD_3 protons of **1** shows a very small chemical shift difference (0.03 ppm; Figure 2; Table I). This could be interpreted in terms of an A orientation of the methyl group or in terms of a fast G to G' equilibration at 104 K. The ^1H chemical shifts of the NCD_2CH_3 group for *all four* subspectra of **2** lie in a narrow δ 1.04–1.09 range. This chemical shift range is typical of an *N*-ethyl methyl group which is oriented gauche to the LP. Thus, the 49% subspectrum reflects an *N*-ethyl methyl group which is undergoing rapid G to G' equilibration at 104 K. The *N*-ethyl methyl is not anti to the LP.

In the 49% sub-spectrum, the C1 methyl protons of **3** show a chemical shift at δ_Z 0.79 (Figure 10; Table V) indicating that the C1 methyl is oriented anti to the LP. If the C1 methyl is anti to the LP, the methine proton (δ_A 2.70) must be gauche to the LP. *Indeed, the small range of chemical shifts for the methine proton in all four sub-spectra (0.27 ppm; Figure 6; Table III) suggests that, in all the NMR-detectable conformations of EMAB, the methine proton is gauche to the LP.* Conformations with the methine proton anti to the LP are not present in concentrations high enough to be NMR-detectable.

In the 49% subspectrum, the C4 methyl protons of the 2-butyl group of **1** show a chemical shift (δ_W 0.96; Table I; Figure 4) in the higher frequency range of the C4 methyl spectrum indicating that the C4 methyl is syn-periplanar to the LP, i.e., in the G' orientation. The C3 methylene protons of the 2-butyl group of **3** show very different scalar coupling with the methine proton ($^3J_{AM}$ = 3 Hz, $^3J_{AO}$ = 12 Hz; Table IV; Figure 9). On the basis of the Karplus relationship, the 49% subspectrum reflects a dominant orientation in which one methylene proton is anti and the other gauche to the methine proton (i.e., G' orientation for the C4 methyl).

Thus, conformations which give rise to the 49% subspectrum must meet specific criteria. For the *N*-ethyl methyl group, there must be comparable populations of G and G' orientations, and the G to G' equilibration is fast at 104 K. The C1 methyl of 2-butyl must be in the A orientation. The C4 methyl is in the G' orientation.

A consideration of models inexorably leads one to the conclusion that only the GAG' and G'AG' conformers of the R_CR_N and S_CS_N stereoisomers satisfy these criteria. The R_CR_N species are shown below. The methine proton is gauche to the ethyl group and the lone pair. This orientation of the methine proton allows the G and G' orientations of *N*-ethyl methyl to be comparably populated and allows averaging of the methylene proton chemical shifts via rapid G to G' equilibration.

(16) Bushweller, C. H.; Lourandos, M. Z.; Brunelle, J. A. *J. Am. Chem. Soc.* **1974**, *96*, 1591.

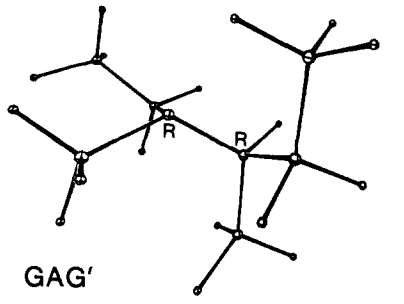

GAG'

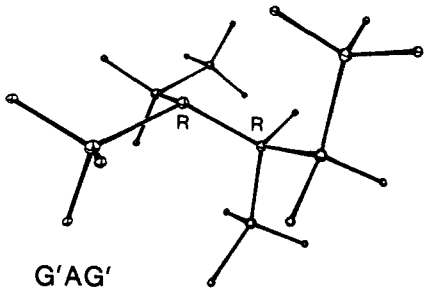

G'AG'

In contrast, the G'AG' conformation of the R_CS_N (or S_CR_N) stereoisomer is significantly destabilized by a syn-periplanar interaction between the *N*-ethyl methyl and the C3 methylene of the 2-butyl group. The R_CS_N GAG' conformation is strongly preferred over the G'AG'. The *N*-ethyl methyl group of the R_CS_N GAG' form is essentially locked in the G orientation, and G to G' equilibration is precluded. One would expect a large chemical shift difference between the NCH_2 protons which is *not* observed in the 49% subspectrum.

12% Subspectrum. Under conditions of slow nitrogen inversion (below 130 K), DNMR simulations show that the 49% subspectrum exchanges magnetization *only* with the 12% subspectrum. The relevant processes involve conformational exchange via rotation about single bonds with no nitrogen inversion occurring (no diastereomeric interconversion). Therefore, the 12% subspectrum must also be due to a conformation or conformations of the R_CR_N and S_CS_N stereoisomers.

The 12% subspectrum of the NCH_2CD_3 group of **1** shows a large chemical shift difference ($\Delta\delta$ 0.79; Figure 2; Table I) indicating that the *N*-ethyl methyl group is locked in the G or G' orientation. Indeed, the NCD_2CH_3 spectrum of **2** at 104 K shows the *N*-ethyl methyl group to be gauche to the LP (vide supra). The chemical shift of the C1 methyl of the 2-butyl group at δ_R 1.15 (Figure 10; Table V) indicates that the C1 methyl is gauche to the LP. The methine proton is also gauche to the LP (vide supra). Therefore, the C3 carbon of the 2-butyl group is anti to the LP. The $^3J_{HH}$ values for coupling of the C3 methylene protons to the methine proton are very different (Figure 9; Table IV) indicating that one methylene proton is predominantly anti and the other gauche to the methine proton. The lower frequency chemical shift of the C4 methyl (δ_Z 0.84) suggests that the C4 methyl is not syn periplanar to the LP.

The only conformation which fits the data above is the GG'G conformation of the R_CR_N and S_CS_N stereoisomers. The R_CR_N conformer is shown below. In the GG'G form, the *N*-ethyl methyl and the C4 methyl groups are both locked in the G orientation. The C1 methyl precludes a G to G' equilibration of the *N*-ethyl methyl group. The *N*-methyl and NCH_2 groups preclude respective G to G' and G to A equilibrations of the C4 methyl.

22% Subspectrum. Having assigned the 49% and 12% subspectra to conformations of the R_CR_N and S_CS_N stereoisomers, the 22% and 17% subspectra must be assigned to conformations of the R_CS_N and S_CR_N stereoisomers.

The 22% subspectrum of the NCH_2CD_3 group of **1** at 104 K shows a large chemical shift difference between the methylene protons ($\Delta\delta$ 0.63; Figure 2; Table I), i.e., a strong preference of methyl for either the G or G' orientation. There is no G to G' equilibration (no averaging). The methyl protons chemical shift

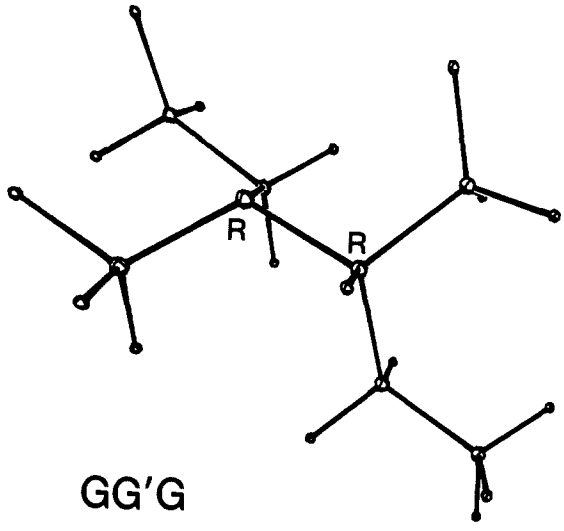

GG'G

of the NCD_2CH_3 group of **2** is in the range δ 1.04–1.09 which is also consistent with a preference for either the G or G' orientation of the *N*-ethyl methyl group. The C1 methyl chemical shift is at δ_X 0.88 (Figure 10; Table V) which indicates that the C1 methyl is anti to the LP (A orientation). The methine proton is gauche to the LP. The C4 methyl of 2-butyl gives a chemical shift in the high frequency region of the C4 methyl spectrum (δ_X 0.95; Table I) indicating that it is syn periplanar with the LP (G' orientation). Again, a large difference between $^3J_{HH}$ values for scalar coupling of the methylene protons to the methine proton (Figure 9; Table IV) indicates a strong preference for an orientation with one methylene proton gauche and the other anti to the methine proton. This is, of course, consistent with a predominant G' orientation of the C4 methyl.

The only conformation which fits the data above is the GAG' form. The S_CR_N species is shown below. In this conformation,

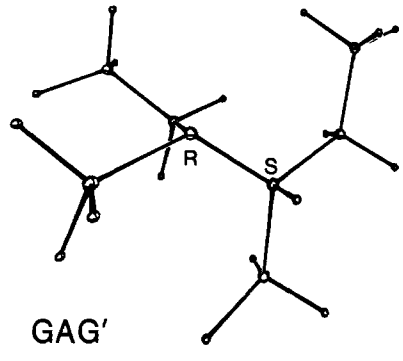

GAG'

the *N*-ethyl methyl adopts the G orientation and is precluded from G to G' equilibration by the C3 methylene of 2-butyl. The C1 methyl is anti to the LP.

17% Subspectrum. In this subspectrum, the chemical shift of the NCD_2CH_3 group of **2** ($\sim\delta$ 1.06) once again indicates a methyl group which is gauche to the LP. The small chemical shift difference between the NCH_2CD_3 protons of **1** ($\Delta\delta$ 0.03 ppm; Figure 2; Table I) indicates rapid G to G' equilibration. The C1 methyl protons of the 2-butyl group give a chemical shift at δ_S 1.12 (Figure 10; Table V) which indicates that the C1 methyl is gauche to the LP. The methine proton is also gauche to the LP (vide supra). The lower frequency chemical shift of the C4 methyl (δ_Y 0.86; Table I) indicates that it is not syn periplanar to the LP. The large difference between $^3J_{HH}$ values for coupling of the methylene protons to the methine proton (Figure 9; Table IV) reveals a strong preference for one methylene proton being gauche and the other anti to the methine proton.

A consideration of models leads one inexorably to assignment of the 17% subspectrum to a system of rapidly interconverting GGG and G'GG conformations. The S_CR_N species are shown below. For these two conformations, a G to G' equilibration for *N*-ethyl methyl is allowed by the positioning of the methine proton.

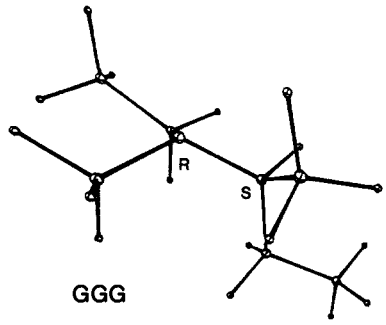

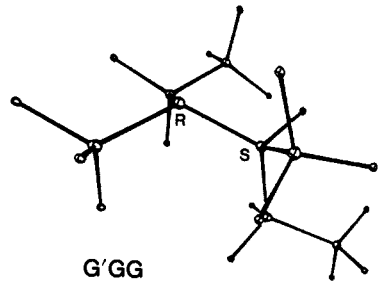

The C1 methyl is gauche to the LP. The 2-butyl C4 methyl is prevented from respective G to A and G to G' equilibrations by the *N*-methyl and *N*-methylene moieties, i.e., the C4 methyl is locked in the G orientation.

Thus, the NMR data indicate the presence of significant populations of the G'AG' and GAG' conformations of the R_CR_N and S_CS_N stereoisomers. The G'AG' and GAG' conformations interconvert via a fast, DNMR-invisible G to G' equilibration of the *N*-ethyl methyl group. The G'AG' and GAG' family of conformations interconverts with the GG'G conformation via a slower, DNMR-visible rotation about the methine carbon–nitrogen bond ($\Delta G^{\ddagger}$ = 6.4 kcal/mol). The R_CR_N and S_CS_N families of conformations are converted respectively to the R_CS_N and S_CR_N families via nitrogen inversion ($\Delta G^{\ddagger}$ = 7.3 kcal/mol). The R_CS_N and S_CR_N families of conformations are dominated by the GAG' species which exchanges via DNMR-visible rotation about the methine carbon–nitrogen bond ($\Delta G^{\ddagger}$ = 5.6 kcal/mol) with a family of rapidly exchanging GGG and G'GG conformations.

It is interesting to note that the NMR data show no evidence for conformations which have the methine proton or the *N*-ethyl methyl group anti to the LP. It is apparent that such conformations are present at concentrations too low to be NMR-detectable.

Molecular Mechanics Calculations. Molecular mechanics calculations were performed on all the staggered conformations of EMAB by using Allinger's 1980 MM2 force field.[17] Geometry optimization was successful for 25 of the 27 conformations for each of the four stereoisomers. The results are summarized in Table VIII. Minimization of the high energy R_CR_N and S_CS_N G'GG' and AG'A conformations as well as the R_CS_N and S_CR_N AGG' and G'AA conformations failed due undoubtedly to the severe nonbonded repulsions.

The enantiomeric R_CR_N and S_CS_N G'AG' conformations are computed to be the most stable (ΔH_f = −27.03 kcal/mol). Compiled in Table VIII are the relative heats of formation of 50 conformations referenced to the R_CR_N and S_CS_N G'AG' forms. In the supplemental Tables IS–IVS, we have also compiled bond angles and dihedral angles for the 50 optimized conformations.

From a perusal of Table VIII, trends are clear. Those conformations which have the methine proton anti to the LP (e.g., R_CR_N GGA; R_CS_N AG'A) are computed to be at least 1.09 kcal/mol less stable than the R_CR_N G'AG' form. Assuming a zero entropy difference between any two conformations, the predicted concentration of the R_CS_N AG'A form at 104 K is a minuscule 0.5% which would effectively render it undetectable by ^{1}H NMR. This is consistent with the NMR data (vide supra). Conformations with a syn periplanar methyl/methyl or methyl/methylene interaction (e.g., R_CR_N GG'G'; R_CS_N G'AG') are at least 2.63 kcal/mol less stable than the R_CR_N G'AG' conformation. Those conformations with two such interactions (e.g., R_CR_N AG'G; R_CS_N G'G'G') are very unstable.

The MM2 force field predicts 18 conformations to have relative energies in the range 0.0–0.8 kcal/mol (Table VIII). Dihedral angles and bond angles for these conformations are compiled in Tables IX and X, respectively. In Tables IX and X (Also Tables IS–IVS), the heavy atoms are numbered according to structure **4**. Assuming that the entropy difference between any two conformations is zero, the calculated percentage of each of the conformations at 104 K is compiled in Table XI.

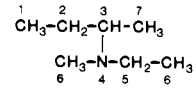

4

Consistent with the NMR data, the MM2 force field predicts the R_CR_N and S_CS_N G'AG' and GAG' family of conformations

Table VIII. Relative Energies of EMAB Conformations Computed by Allinger's 1980 MM2 Force Field

R_CR_N or S_CS_N conformation	rel energy, kcal/mol	R_CS_N or S_CR_N conformation	rel energy, kcal/mol
G'AG'	0.00	GAG'	0.08
GAG'	0.17	G'GG	0.50
G'AG	0.61	GAG	0.73
GG'G	0.67	GGG	0.76
GAG	0.82	AG'A	1.09
GGA	1.10	GG'A	1.11
AGA	1.11	AG'G	1.83
AGG	1.81	GG'G	2.23
GGG	2.23	G'AG'	2.63
GG'G'	2.86	GGG'	2.95
G'G'G	2.95	G'GG'	2.99
GGG'	3.32	AG'G'	3.17
AGG'	3.40	G'AG	3.19
G'AA	3.40	AAG'	3.27
AAG'	3.49	GG'G'	3.31
GG'A	3.69	G'GA	3.51
GAA	3.74	GGA	3.66
AG'G	3.87	AGG	3.73
AAG	4.09	AAG	3.84
G'G'G'	4.81	G'G'A	4.10
G'GA	4.96	GAA	4.47
G'GG	5.14	G'G'G	5.01
AG'G'	6.15	G'G'G'	6.25
G'G'A	6.35	AAA	6.49
AAA	6.43	AGA	6.71
G'GG'	***	AGG'	***
AG'A	***	G'AA	***

Table IX. Dihedral Angles for Selected Stable Conformations of EMAB Computed by Allinger's 1980 MM2 Force Field

	dihedral angles[a]		
	C_1–C_2–C_3–N_4	C_2–C_3–N_4–C_5	C_3–N_4–C_5–C_6
	R_CR_N or S_CS_N Conformer		
G'AG'	52.8	−172.4	55.6
GAG'	51.0	−167.6	169.3
G'AG	162.2	−172.1	54.8
GG'G	172.4	61.5	172.7
GAG	161.8	−166.3	169.0
	R_CS_N or S_CR_N Conformer		
GAG'	−51.7	−64.6	173.5
G'GG	−173.9	60.7	54.8
GAG	−162.6	−66.2	174.1
GGG	−174.6	65.8	168.5

[a] See structure **4** in the text for numbering of heavy atoms. For the dihedral angle A–B–C–D, when looking down the B–C bond, the sign of the angle is negative if D is moved counterclockwise to eclipse A and positive if clockwise.

(17) Allinger, N. L.; Yuh, Y. H. *QCPE* **1980**, 395.

Table X. Bond Angles for Selected Stable Conformations of EMAB Computed by Allinger's 1980 MM2 Force Field

	bond angles[a]		
	C_3–N_4–C_5	C_3–N_4–C_8	C_5–N_4–C_8
	R_CR_N or S_CS_N Conformer		
G'AG'	113.9	113.2	109.1
GAG'	111.9	113.2	111.0
G'AG	114.1	113.1	109.2
GG'G	113.4	111.8	111.1
GAG	112.0	113.1	111.1
	R_CS_N or S_CR_N Conformer		
GAG'	113.6	111.5	111.1
G'GG	114.3	113.1	109.2
GAG	114.1	112.2	109.8
GGG	112.2	113.1	111.1

[a] See structure **4** in text for numbering of heavy atoms.

Table XI. MM2 Relative Energies and Calculated Percentages of Stable Conformations of EMAB at 104 K

	rel energy, kcal/mol	%age at 104 K[a]
	R_CR_N or S_CS_N Conformer	
G'AG'	0.00	42
GAG'	0.17	18
G'AG	0.61	2
GAG	0.82	1
GG'G	0.67	2
	R_CS_N or S_CR_N Conformer	
GAG'	0.08	29
GAG	0.73	1
G'GG	0.50	4
GGG	0.76	1

[a] Calculated by assuming a zero entropy difference between any two conformations.

to be dominant. An MM2 dihedral angle driver calculation for a direct G'AG' to GAG' exchange gave a barrier of 4.4 kcal/mol which is too low to be DNMR-visible even at 104 K.[17] Thus, consistent with the NMR data, the R_CR_N and S_CS_N G'AG' and GAG' conformations are predicted to exchange rapidly on the ^1H NMR chemical exchange time scale even at 104 K. The G'AG' and GAG' species can interconvert, respectively, with small amounts of the G'AG and GAG forms via rotation about the C2–C3 bond of the 2-butyl group. An MM2 dihedral angle driver calculation predicts a DNMR-invisible 4.0 kcal/mol barrier for this process. The G'AG and GAG forms can in turn interconvert via a DNMR-invisible G to G' equilibration of the *N*-ethyl methyl. Thus, the G'AG', GAG', G'AG, and GAG forms constitute a family of rapidly exchanging conformations of the R_CR_N and S_CS_N stereoisomers (Scheme I). This family of conformations is dominated by the G'AG' and GAG' forms. The total percentage of all four species estimated from the MM2 calculations (63%; Table XI) is in reasonable agreement with the NMR measurement (49%) at 104 K (Tables I, III–V).

In Scheme I, the rapidly interconverting R_CR_N G'AG', GAG', G'AG, and GAG conformations are enclosed in a box delineated by dashed lines. If a dashed line box in Scheme I contains more than one conformation, the implication is that any conformations within the box interconvert at a rate which is fast on the NMR chemical exchange time scale at 104 K. A box delineated by a solid line is meant to enclose all the NMR-detectable conformations of one diastereomer. Interconversion of conformations between different dashed line boxes within a solid line box occurs by isolated rotation about the methine carbon–nitrogen bond. The upper solid line box in Scheme I includes all the NMR-detectable conformations of the R_CR_N stereoisomer; the lower solid line box the R_CS_N diastereomer. Interconversion between solid line boxes requires nitrogen inversion (diastereomeric interconversion).

Within the R_CR_N and S_CS_N families of conformations, the GG'G conformation is the only remaining conformation to have an MM2 relative energy less than 0.8 kcal/mol (Table XI). Conversion of the G'AG', GAG', G'AG, GAG family of conformations to the GG'G form does involve a DNMR-visible rotation about the methine carbon–nitrogen bond (Scheme I; rate constant k_2). Indeed, the NMR parameters associated with the 12% subspectra of **1**, **2**, and **3** require assignment to the GG'G conformation (vide supra). The estimated percentage of the GG'G form at 104 K from the MM2 data is 2%. The free energy of activation ($\Delta G^\ddagger$) for conversion of the G'AG', GAG', G'AG, and GAG family of conformations to the GG'G form is 6.4 ± 0.2 kcal/mol at 122 K (Tables II, VI).

For the R_CS_N and S_CR_N families of conformations, the MM2 force field predicts the GAG' conformation to be most stable (Table XI). The GAG' conformation interconverts with the substantially less stable GAG form via a low-barrier DNMR-invisible rotation about the C2–C3 bond of the 2-butyl group (Scheme I). The two remaining stable conformations (i.e., relative MM2 energy <0.8 kcal/mol) are the GGG and G'GG species (Scheme I). These two conformations of comparable energy interconvert via a DNMR-invisible G to G' equilibration of the *N*-ethyl methyl group. The GAG' and GAG family is converted to the GGG and G'GG family via a higher barrier, *DNMR-visible* rotation about the methine carbon–nitrogen bond, which corresponds to interconversion between the 22% and 17% subspectra. As deduced from the NMR data above, the 22% subspectrum is dominated by the GAG' species, and the 17% subspectrum indicates rapid equilibration between comparable populations of the GGG and G'GG conformations. Thus, the MM2 calculations agree well with NMR data. The $\Delta G^\ddagger$ for conversion of the GAG' and GAG family to the GGG and G'GG ensemble is 5.6 ± 0.2 kcal/mol at 122 K. The DNMR $\Delta G^\ddagger$ for nitrogen inversion (i.e., R_CR_N to R_CS_N or S_CR_N to S_CS_N diastereomeric conversion) is 7.3 ± 0.2 kcal/mol at 147 K.

Summary

The stereodynamics of *N*-ethyl-*N*-methyl-2-aminobutane (EMAB) is effectively summarized in Scheme I. For the R_CR_N (or S_CS_N) stereoisomer, there are two families of conformations which have populations of 49% and 12% at 104 K. One family (49%) contains the G'AG', GAG', G'AG, and GAG species which interconvert rapidly on the NMR chemical exchange time scale even at 104 K. Both NMR data and molecular mechanics calculations indicate that this family is dominated by the G'AG' and GAG' species. This family of conformations converts to the GG'G species (12%) via a DNMR-visible rotation about the methine carbon–nitrogen bond ($\Delta G^\ddagger$ = 6.4 kcal/mol). Inversion at nitrogen will convert the R_CR_N (or S_CS_N) family of conformations to the diastereomeric R_CS_N (or S_CR_N) species ($\Delta G^\ddagger$ = 7.3 kcal/mol) which also show two NMR-detectable, comparably populated families of conformations. One family contains the dominant GAG' conformation which interconverts with the substantially less stable GAG form at a rapid rate at 104 K. This family is converted via a DNMR-visible rotation about the methine carbon–nitrogen bond to the comparably populated and rapidly interconverting GGG and G'GG species.

In the most stable conformations (e.g., R_CR_N G'AG' and GAG'; R_CS_N GAG'), there are similarities. The *N*-ethyl methyl group is gauche to the nitrogen lone pair. The C1 methyl of 2-butyl is anti to the lone pair. The C4 methyl of 2-butyl is syn periplanar to the lone pair. The methine proton is gauche to the lone pair. There is no evidence in the NMR spectra for conformations which have the methine proton or the *N*-ethyl methyl group anti to the lone pair.

It might be expected that the stereodynamics of EMAB discovered in these studies is representative of any chiral amine which has one methyl, one primary, and one secondary alkyl group bonded to nitrogen.

Experimental Section

NMR spectra were run on a Bruker WM250 pulsed FT NMR system at the University of Vermont. Temperature measurement is accurate to ±3 K. For this reason, we report only $\Delta G^\ddagger$ values from DNMR line shape analysis and do not report $\Delta H^\ddagger$ and $\Delta S^\ddagger$ values which are subject

Scheme I. Stable Equilibrium Conformations of the R_CR_N and R_CS_N Diastereomers of EMAB[a]

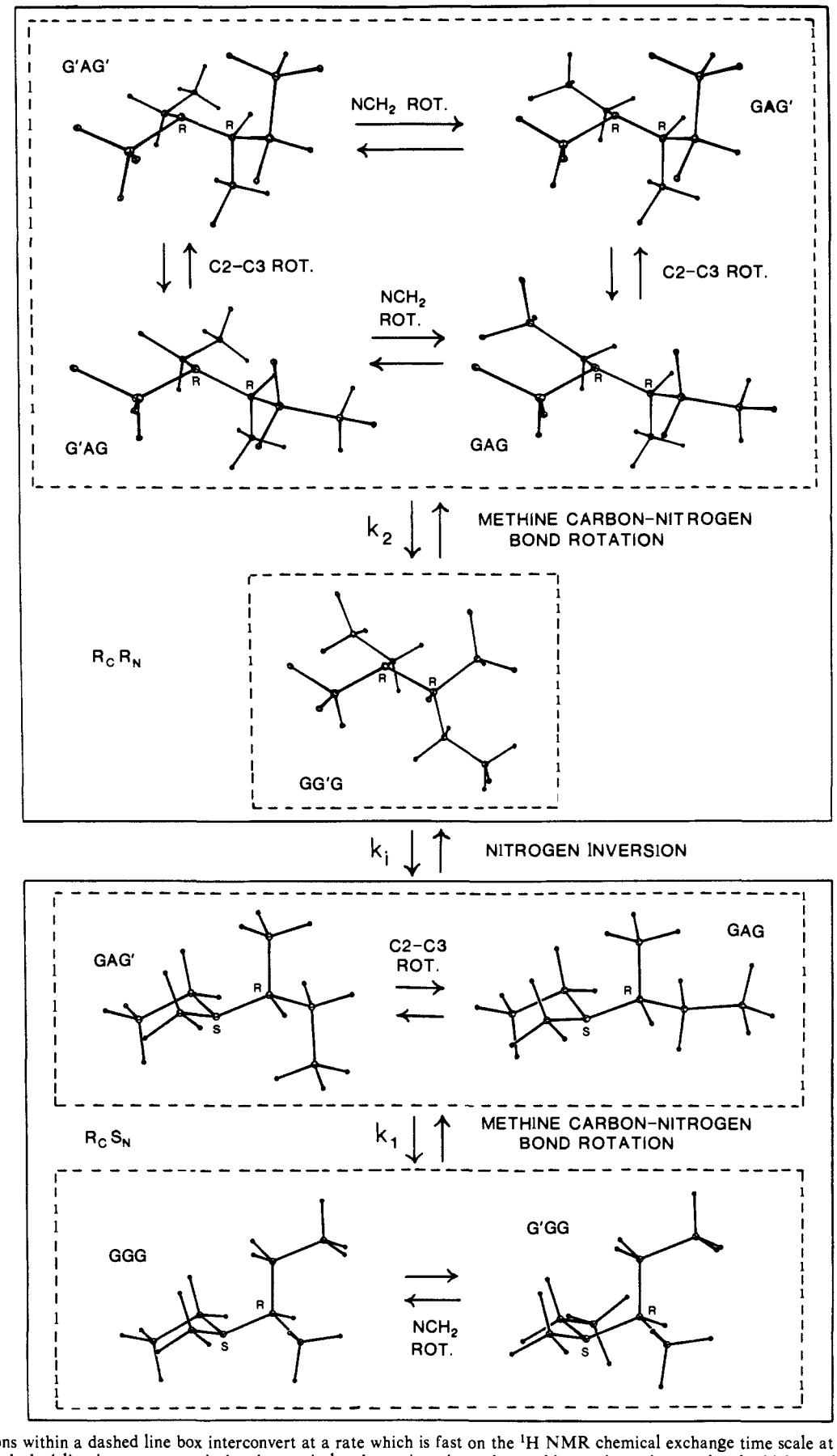

[a] Conformations within a dashed line box interconvert at a rate which is fast on the ^1H NMR chemical exchange time scale at 104 K. Interconversion between dashed line boxes occurs via barriers to isolated rotation about the methine carbon–nitrogen bond which are high enough to be DNMR-visible. Interconversion between solid line boxes occurs via nitrogen inversion (diastereomeric interconversion) which also has a barrier high enough to be DNMR-visible.

to systematic errors. Samples were prepared in precision NMR tubes, degassed three times, and sealed.

2-Butanone-*1,1,1,3,3-d*$_5$. 2-Butanone (10 mL; Aldrich Chemical Co.), Na_2CO_3 (0.1 g), and D_2O (20 mL; Aldrich Chemical Co.) were placed into a 100-mL flask equipped with a stirring bar, reflux condenser, and drying tube. The mixture was allowed to reflux for 24 h at which time the 2-butanone was separated from the D_2O by salting out and distilling. The exchange procedure was performed five times. NMR analysis revealed 99.7% deuterium incorporation.

Methylamine-*N,N-d*$_2$ Deuteriochloride. Methylamine hydrochloride (50.0 g; Pfalz and Bauer, Inc.), and D_2O (50 mL; Aldrich Chemical Co.) were placed in a flask equipped with a stirring bar, reflux condenser, and drying tube. The mixture was refluxed for 24 h at which time the D_2O was removed at reduced pressure. The exchange procedure was performed six times. NMR analysis revealed 99.5% deuterium incorporation.

***N*-Methyl-2-aminobutane-*1,1,1,2,3,3-d*$_6$.** 2-Butanone-*1,1,1,3,3-d*$_5$ (2.69 mL), methylamine-*N,N-d*$_2$ deuteriochloride (10.13 g), and sodium cyanoborodeuteride (1.88 g; Aldrich Chemical Co.) in 75 mL of methanol-d_1 were stirred for 72 h at 298 K. The solution was cooled while concentrated HCl was added until the pH was less than 2. The methanol was removed by distillation. The residue was taken up in 10 mL of water and extracted with 20-mL portions of ether. The aqueous solution was cooled and brought to a pH greater than 10 with solid KOH, saturated with NaCl, and extracted with five 15-mL portions of ether. The combined extracts were dried ($MgSO_4$), and the ether was removed on the spinning band column. The residue was distilled with a short path column (yield: 1.5 g; 57.5%). Characterization was done by ^{1}H NMR.

***N*-Methyl-*d*$_3$-2-aminobutane-*4,4,4-d*$_3$** was prepared by the same procedure used for *N*-methyl-2-aminobutane-*1,1,1,2,3,3-d*$_6$, except that 2-butanone-*4,4,4-d*$_3$ (2.69 mL; MSD Isotopes), methyl-d_3-amine hydrochloride (10.125 g; Aldrich Chemical Co.), sodium cyanoborohydride (1.88 g; Aldrich Chemical Co.), and methanol were used.

***N*-Methyl-2-aminobutane-*1,1,1,3,3-d*$_5$** was prepared by the same procedure used for *N*-methyl-2-aminobutane-*1,1,1,2,3,3-d*$_6$, except that sodium cyanoborohydride (1.88 g; Aldrich Chemical Co.) was used.

***N*-Ethyl-*2,2,2-d*$_3$-*N*-methyl-*d*$_3$-2-aminobutane-*1,1,1,2,3,3-d*$_6$ (1).** Benzene (1 mL) and 50% NaOH (4 mL) were added to a 10-mL round-bottom flask equipped with a magnetic stirring bar and stopper. *N*-Methyl-d_3-2-aminobutane-*1,1,1,2,3,3-d*$_6$ (2.0 mL, 0.006 mol) and iodoethane-*2,2,2-d*$_3$ (1 g, 0.006 mol; MSD Isotopes) were added to the benzene layer. The reaction mixture was stirred for 72 h. The reaction mixture was then poured into a test tube and centrifuged, and the clear layer was removed by pipette. The product was purified on a 5% XE-60/25% SF-96 Chromosorb W GLPC column (20 ft by 3/8 in.). Characterization was done by ^{1}H NMR, mass spectrometry, and comparison of the GC retention time with that of the non-deuteriated compound. ^{1}H NMR: See Figures 1–4 and Table I.

***N*-Ethyl-*1,1-d*$_2$-*N*-methyl-2-aminobutane-*1,1,1,3,3-d*$_5$ (2)** was prepared by the same procedure used for **1** except that *N*-methyl-2-aminobutane-*1,1,1,3,3-d*$_5$ (2.0 mL, 0.006 mol) and iodoethane-*1,1-d*$_2$ (1 g, 0.006 mol; MSD Isotopes) were used. Characterization was done by ^{1}H NMR, mass spectrometry, and comparison of the GC retention time with that of the all hydrogen compound. ^{1}H NMR: See Figures 5 and 6 and Table III.

***N*-Ethyl-*d*$_5$-*N*-methyl-*d*$_3$-2-aminobutane-*4,4,4-d*$_3$ (3)** was prepared by the same procedure used for **1** except that *N*-methyl-d_3-2-aminobutane-*4,4,4-d*$_3$ (2.0 mL, 0.006 mol) and iodoethane-d_5 (1 g, 0.006 mol; MSD Isotopes) were used. Characterization was done by ^{1}H NMR, mass spectrometry, and comparison of the GC retention time with that of the all-hydrogen compound. ^{1}H NMR: See Figures 7–10 and Tables IV and V.

Acknowledgment. C.H.B. is grateful to the National Science Foundation for support (Grant CHE80-24931 and CHE83-06876). We appreciate the assistance of the University of Vermont Academic Computing Center staff in providing outstanding computational support. We also appreciate assistance with the molecular mechanics calculations from Christine Dimeglio.

Supplementary Material Available: Tables of bond angles and dihedral angles for the R_CR_N/S_CS_N and R_CS_N/S_CR_N families of conformations calculated by using Allinger's 1980 MM2 molecular mechanics force field (4 pages). Ordering information is given on any current masthead page.

Intermolecular Electronic Interactions in the Primary Charge Separation in Bacterial Photosynthesis

M. Plato,[†] K. Möbius,[†] M. E. Michel-Beyerle,[‡] M. Bixon,[§] and Joshua Jortner*,[§]

Contribution from the Institut für Molekülphysik, Freie Universität Berlin, Arnimallee 14, 1000 Berlin 33, FRG, and Institut für Physikalische und Theoretische Chemie, Technische Universität München, Lichtenbergstrasse 4, Garching, FRG, and the School of Chemistry, Sackler Faculty of Exact Sciences, Tel Aviv University, 69 978 Tel Aviv, Israel.
Received November 24, 1987

Abstract: In this paper we utilize the intermolecular overlap approximation to calculate the relative magnitudes of the electronic transfer integrals between the excited singlet state (^{1}P*) of the bacteriochlorophyll dimer (P) and the accessory bacteriochlorophyll (B) and between B$^-$ and bacteriopheopytin (H), along the L and M subunits of the reaction center (RC) of *Rps. viridis*. The ratio of the electron-transfer integrals for $B_L^-H_L-B_LH_L^-$ and for $B_M^-H_M-B_MH_M^-$ was calculated to be 2.1 ± 0.5, which together with the value of 2.8 ± 0.7 for the ratio of the transfer integrals for $^1P^*B_L-P^+B_L^-$ and for $^1P^*B_M-P^+B_M^-$ results in the electronic contribution of 33 ± 16 to the ratio k_L/k_m of the rate constants k_L and k_M for the primary charge separation across the L and M branches of the RC, respectively. The asymmetry of the electronic coupling terms, which originates from the combination of the asymmetry in the charge distribution of ^{1}P* and of structural asymmetry of the P–B and B–H arrangements across the L and M subunits, provides a major contribution to the unidirectionality of the charge separation in bacterial photosynthesis. A significant contribution to the transfer integrals between adjacent pigments originates from nearby methyl groups through hyperconjugation. The ratio 6 ± 2 of the transfer integrals for $^1P^*B_L-P^+B_L^-$ and for $B_L^-H_L-B_LH_L^-$ was utilized to estimate the energetic parameters required to ensure the dominance of the superexchange mediated unistep electron transfer $^1P^*BH \rightarrow P^+BH^-$ over the thermally activated $^1P^*B \rightarrow P^+B^-$ process.

I. Introduction

The conversion of solar energy into photochemical energy in reaction centers (RC) of photosynthetic bacteria proceeds via a sequence of well-organized, highly efficient, directional, and specific electron-transfer steps across the photosynthetic membrane.[1-3] The electron-transfer processes involve various pigments

[†] Institut für Molekülphysik, Freie Universität Berlin.
[‡] Institut für Physikalische und Theoretische Chemie, Technische Universität München.
[§] Tel Aviv University.

(1) Deisenhofer, J.; Epp, O.; Miki, K.; Huber, R.; Michel, H. *J. Mol. Biol.* **1984**, *180*, 385.
(2) Deisenhofer, J.; Epp, O.; Miki, K.; Huber, R.; Michel, H. *Nature (London)* **1985**, *318*, 618.

0002-7863/88/1510-7279$01.50/0 © 1988 American Chemical Society